DOI: 10.2507/37th.daaam.proceedings.xxx

SYMBOLIC REGRESSION ANALYSIS OF STRAIN RATE-DEPENDENT FFF-PRINTED STRONGMAN MATERIAL

Ajdin Vatres, Kemal Hamzic* & Adi Pandzic

Working Paper of 37th DAAAM Symposium

This Publication has to be referred as: Vatres, A[jdin]; Hamzic, K[emal] & Pandzic, A[di] (2026). Title of Paper, Proceedings of the 37th DAAAM International Symposium, pp.xxxx-xxxx, B. Katalinic (Ed.), Published by DAAAM International, ISBN 978-3-902734-xx-x, ISSN 1726-9679, Vienna, Austria
DOI: 10.2507/37th.daaam.proceedings.xxx

Abstract

Strain rate-dependent mechanical behaviour of FFF-printed Strongman (STR) material was experimentally investigated at several strain rates. Identification of relationships between material properties and process parameters increasingly relies on machine learning methods. Although resulting models demonstrate good predictive performance, they typically lack physical interpretability and require substantial data. To address these limitations, this study presents a hybrid approach that combines symbolic regression with a modified constitutive Cingara equation. Baseline constitutive formulation was selected based on the characteristic initial hardening and peak stress response observed in the experimental stress strain curves. Since the original formulation does not fully describe the subsequent stationary response, symbolic regression was employed to identify a corrective residual term. When evaluated on the STR material proposed model achieved a mean squared error (MSE) of 3.044, a mean absolute error (MAE) of 1.325 and a coefficient of determination (R^2) of 0.978. Results demonstrate that the proposed approach achieves high predictive accuracy while maintaining a physically interpretable model structure.

Keywords: Additive manufacturing; Strain rate dependence; Symbolic regression; Cingara equation.

1. Introduction

Additive manufacturing (AM) has become an important manufacturing technology due to its ability to produce complex geometries, reduce material waste, enable product customisation and manufacture structures that are difficult to produce using conventional methods. Its application has expanded from rapid prototyping to functional components in areas such as aerospace, biomedical engineering, automotive applications and construction [1]. Among different AM technologies, fused filament fabrication (FFF) is widely used for polymer components, where a thermoplastic filament is deposited layer by layer to form the final geometry [1], [2]. Mechanical behaviour of FFF-printed parts is affected by several manufacturing parameters, including layer thickness, infill density, infill pattern, printing orientation and printing conditions [1], [3].

Mechanical characterization of FFF-printed polymers is therefore important for their use in engineering applications. In addition to manufacturing parameters loading conditions can influence the measured material response. Polymer materials can exhibit rate-dependent behaviour, meaning that the stress strain response can change with the applied strain rate.

Strain rate is an important parameter in the mechanical characterization of FFF-printed polymers. Investigating PLA, Tough-PLA and carbon-fibre-reinforced PLA at five different strain rates showed that strain rate affects tensile strength, yield strength, Young's modulus and strain, with the magnitude and trend of the response depending on the material. These results demonstrate that mechanical characterization at a single loading rate may not be sufficient when the material is intended for applications involving different loading conditions [4].

This strain rate-dependant behaviour has been reported for conventional thermoplastics as well as additively manufactured polymers. For polypropylene, strain rate-dependent tensile behaviour was investigated using an analytical constitutive approach based on a Burgers model, demonstrating the need to account for loading rate when describing the mechanical response of thermoplastic polymers [5]. Similar behaviour was reported for self-reinforced polypropylene and polyethylene terephthalate where stress strain curves were obtained at different strain rates and a modified G'Sell–Jonas model was developed to describe the rate-dependent response [6].

Such an approach shows that experimental testing at different strain rates is not only useful for describing the material response, but also provides the data required for developing a constitutive relation that can be used beyond the individual tensile or compression tests. When several strain rates are considered simultaneously, however, the modelling problem becomes more demanding, since the model must describe both the dependence on strain and the dependence on strain rate.

Another DAAAM study demonstrated the use of regression-based parameter identification for modelling the time-dependent behaviour of a 3D-printed polymer. Authors investigated ABS plastic and determined the parameters of a Prony-series model using the least-squares method and its variations showing how experimental data can be used to identify the parameters of an analytical constitutive formulation [7].

Symbolic regression has also been used for constitutive material modelling. It can be applied either to identify parameters of an existing constitutive model or to derive a constitutive equation directly from experimental data. Both approaches were tested using compression data obtained under different processing conditions and the resulting models were implemented in finite-element simulations. This shows that symbolic regression can provide explicit mathematical expressions while maintaining good predictive capability, which makes it suitable for developing interpretable constitutive models [8].

A further development of this concept is to retain an existing constitutive formulation and use symbolic regression to extend its dependence on processing variables. A genetic-programming approach was proposed in which the functional dependence of constitutive calibration parameters on processing conditions, including deformation temperature and strain rate was identified from experimental data. Instead of replacing the complete physics-based formulation, derived expressions were used to replace or extend selected calibration parameters allowing the constitutive model to describe intermediate processing conditions. This approach demonstrates that symbolic regression can be used in combination with an existing constitutive structure rather than necessarily replacing it with a fully data-driven model [9].

Related modelling strategy was recently presented by Mao et al. who combined a conventional constitutive formulation with a data-driven approach for predicting the hot deformation behaviour of 12Cr2Mo1V steel. Cingara empirical equation was used as the analytical basis for describing the flow behaviour before the peak stress, while a GA-BP neural network was used to determine and optimise the constitutive parameters. Predicted parameters were subsequently substituted into the analytical constitutive equations to reconstruct the complete flow stress curves. This study demonstrates that an existing constitutive equation can be retained as the structural basis of a model, while a data-driven method can be used to improve its description of material behaviour [10].

A similar principle is adopted in the present study, but with symbolic regression used instead of a neural network and with the modelling objective focused on strain rate-dependent tensile behaviour of FFF-printed STR material. Rather than replacing the complete constitutive formulation, a modified Cingara-type equation is first used as a baseline model. Symbolic regression is then applied to the residual between the experimental data and the baseline prediction resulting in an explicit correction term. Final formulation therefore combines the analytical structure of the baseline constitutive equation with a symbolic data-driven correction.

Symbolic regression has also been applied to nonlinear polymer and elastomer constitutive modelling. A procedure was developed for automatically generating interpretable hyperelastic material models in the form of algebraic expressions. Approach was first tested on predefined generalized Mooney-Rivlin models and was subsequently applied to experimental data for vulcanized rubber and a temperature dependent thermoplastic polyester elastomer. Resulting expressions showed good agreement with experimental data and were formulated in a way that allowed direct implementation in finite element procedures [11].

These studies indicate several possible approaches for constitutive modelling of rate-dependent polymeric materials. Conventional approach is to select a predefined constitutive equation and calibrate its parameters independently for each strain rate. A more flexible approach is to formulate the material response directly as a data-driven function of strain and strain rate. Symbolic regression provides another possibility, since it can generate an explicit mathematical relationship while maintaining a direct connection between the input variables and the predicted stress. For materials such as FFF-printed STR, where the stress strain response changes with strain rate, a model of the form $\sigma = f(\varepsilon, \dot{\varepsilon})$ is desirable because it can represent several experimental conditions within a single formulation. However, directly searching for the complete constitutive equation may result in unnecessarily complex expressions. A hybrid strategy, in which a physically or empirically motivated baseline equation is combined with a symbolic correction can retain the main structure of the material response while allowing additional rate and strain-dependent effects to be identified from experimental data.

Working Paper of 37th DAAAM Symposium

Based on this concept, present study investigates the strain rate-dependent tensile behaviour of FFF-printed STR material and develops a unified constitutive model covering the investigated strain-rate range. Experimental stress strain data obtained at several strain rates are first used to establish a baseline constitutive formulation. Symbolic regression is subsequently applied to the residual between the experimental response and the baseline model resulting in a correction term that extends the original formulation. Final equation therefore combines an analytical baseline with a symbolic data-driven correction providing an explicit expression for stress as a function of strain and strain rate.

2. Materials and methods

PLA-Strongman is a high-performance PLA based material developed for applications requiring higher toughness and impact resistance than conventional PLA, while maintaining good printability. Its tensile mechanical properties have been investigated for FFF-printed specimens under different infill conditions, showing that the material can be used for components where higher mechanical resistance is required [12].
Experimental data used in this study were obtained from tensile tests on FFF-printed STR material at four strain rates, 0.0005, 0.002, 0.02, and 0.1 s^{-1}, as described in our previous work [13]. Data were reanalysed in the present study using symbolic regression to develop a unified mathematical model.
Number of points n, minimum strain ε_{min}, maximum strain ε_{max}, strain at maximum stress $\varepsilon_{\sigma_{max}}$, minimum stress σ_{min} and maximum stress are given σ_{max} in Table 1.

$\dot{\varepsilon}$	n	ε_{min}	ε_{max}	$\varepsilon_{\sigma_{max}}$	σ_{min}	σ_{max}
0.0005	81	0.00	7.94	2.30	0.00	37.61
0.002	72	0.00	7.10	2.30	0.00	39.27
0.02	76	0.00	7.50	3.80	0.00	42.32
0.1	68	0.00	6.64	4.60	0.00	48.60

Table 1. Summary of stress strain data and characteristic values at different strain rates

To ensure uniform representation across deformation rates and prevent implicit weighting of individual rates, the dataset was constructed with an equal number of samples for each deformation rate. Each curve was resampled to 100 uniformly spaced points, with intermediate values determined by linear interpolation. The final pre-processed curves are given in Fig. 1.

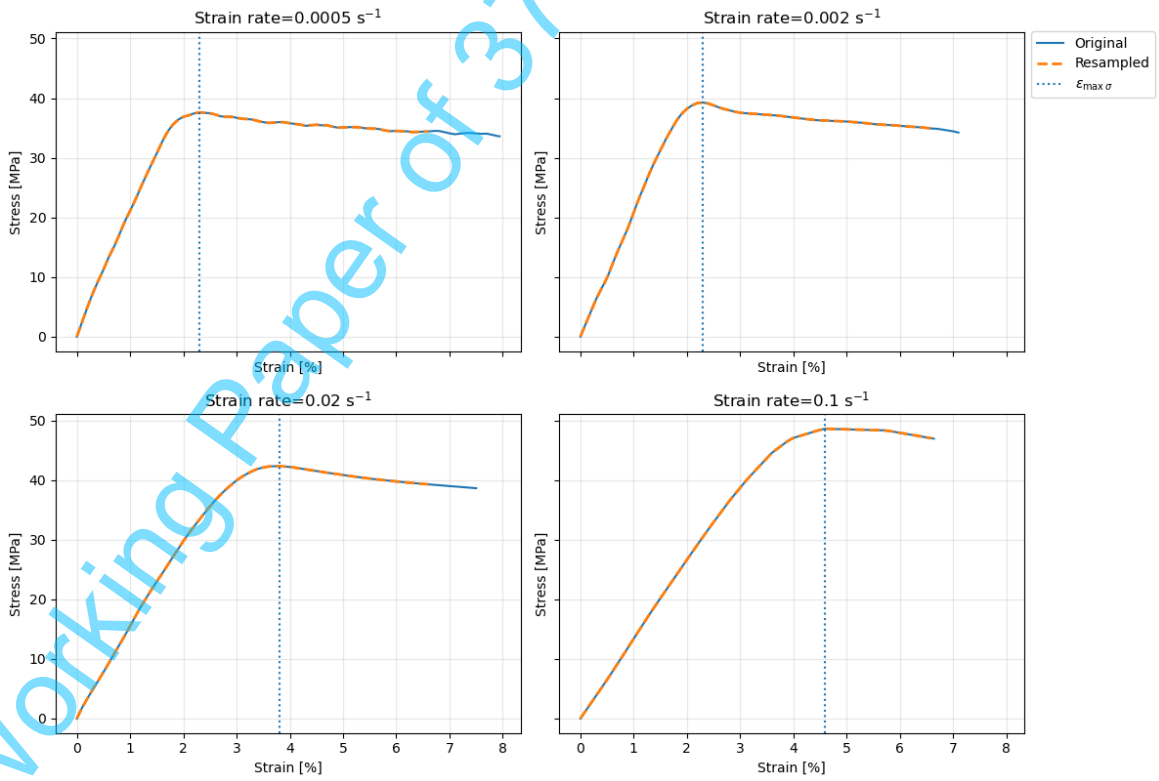

Fig. 1. Resampled stress strain curves at different strain rates

Working Paper of 37th DAAAM Symposium

Symbolic regression (SR) is a supervised learning method capable of generating interpretable predictive models. Given some dataset $\mathcal{D} = \{(x_i, y_i)\}_{i=1}^{n}$, with x_i, and y_i being the input vector and model output, SR finds the function f that minimizes some predefined (often multitask) loss function $\mathcal{L}$ [14], [15]:

$$\mathcal{L}(f) = \sum_{i=1}^{n} \mathcal{L}(f(x_i), y_i) \tag{1}$$

Unlike most conventional machine learning (ML) methods, SR does not require the functional form of the model to be specified a priori. Rather the form is learned through the optimization process and is represented by a closed form mathematical expression stated in Equation 1 [16]. Space of candidate functions is typically defined by a set of allowable primitives including operators, elementary functions, variables and constants, which are combined to construct mathematical expressions. These expressions are commonly represented as binary trees in which each internal node corresponds to a mathematical operation and each leaf node represents an input variable or constant. Optimization process therefore performs combinatorial search over possible tree structures and their associated parameters to identify an expression that provides an optimal balance between predictive accuracy and model complexity [17]. Multiple ways of performing this search exist with associated frameworks. In this work we chose to use evolutionary algorithms implemented with the frameworks PySR and SymbolicRegression.jl [15]. Schematic representation of SR is given in Fig. 2.

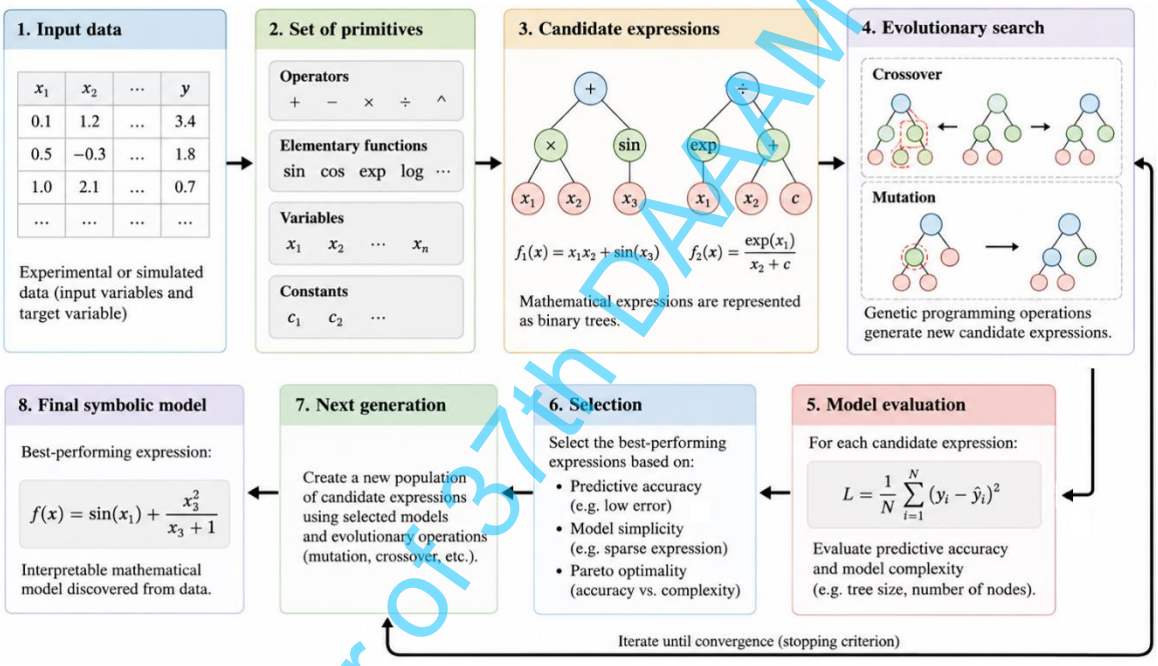

Fig. 2. Schematic representation of the symbolic regression (SR) workflow

Cingara constitutive model used in this study was originally developed to describe high temperature flow curves of stainless steel. This model is given by Equation 2 [18].

$$\frac{\sigma}{\sigma_{max}} = \left[\left(\frac{\varepsilon}{\varepsilon_{\sigma_{max}}}\right) e^{\left(1-\frac{\varepsilon}{\varepsilon_{\sigma_{max}}}\right)}\right]^{c} \tag{2}$$

were c is a material dependent constant that varies with temperature and strain rate. Original formulation provides an accurate description of the stress strain response up to the maximum stress σ_{max}, while present work extends the formulation to account for the subsequent response as well.

Flow behavior where this model has been successfully applied is characterized by competing work hardening and dynamic softening resulting in distinct regimes in the stress strain curves. During the initial phase there is linear increase in stress. As strain continues to increase a critical point is reached at which the curves slope begins to decrease to the point of peak stress σ_{max}. Beyond this point dynamic softening can become dominant leading to an inversion of the curves slope. Finaly dynamic equilibrium can be achieved leading to a near steady state regime [10]. While the underlining deformation mechanism governing high temperature steel flow differ from STR material, stress strain curves shown in Fig. 1 exhibit qualitatively similar characteristics, including an initial hardening regime, a distinct peak stress and a subsequent near-steady-state response. This similarity motivates the use of a Cingara based formulation as a physically informed baseline model for the STR material (Equations 3, 4 and 5).

Working Paper of 37th DAAAM Symposium

$$\sigma(\dot{\varepsilon},\varepsilon) = a(\dot{\varepsilon})\varepsilon e^{-\frac{\varepsilon}{c(\dot{\varepsilon})}} \quad (3)$$

$$a(\dot{\varepsilon}) = a_0 + a_1 \log \dot{\varepsilon} \quad (4)$$

$$c(\dot{\varepsilon}) = c_0 + c_1 \dot{\varepsilon} \quad (5)$$

This study proposes a hybrid model comprising a physically informed baseline model $\sigma(\dot{\varepsilon},\varepsilon)$ and a SR model $f^*(\dot{\varepsilon},\varepsilon)$ trained to predict the residuals of the baseline formulation. Resulting prediction $\hat{\sigma}$ is given by Equations 6 and 7 were σ_{epx} are the experimentally measured stress values.

$$\hat{\sigma}(\dot{\varepsilon},\varepsilon) = \sigma(\dot{\varepsilon},\varepsilon) + f^*(\dot{\varepsilon},\varepsilon) \quad (6)$$

$$f^* = \underset{f\in\mathcal{F}}{\operatorname{argmin}}\, \mathcal{L}(\sigma_{epx}(\dot{\varepsilon},\varepsilon) - (\sigma(\dot{\varepsilon},\varepsilon) + f^*(\dot{\varepsilon},\varepsilon))) \quad (7)$$

3. Results and discussion

Symbolic regression models were developed using the PySR package. Optimization was performed for 2000 iterations using 30 initial populations each consisting of 60 individuals. Operator set comprised four binary operators (addition, subtraction, multiplication, and division) and five unary operators (exponential, logarithm, square, sine and cosine). To promote model interpretability and limit expression complexity, maximum tree size was restricted to 25 for the full symbolic regression model and to 10 for the residual model.
Baseline constitutive model was calibrated using nonlinear least-squares optimization implemented through the SciPy package. All models were trained on a workstation equipped with an AMD Ryzen 7 5800H processor.
Mathematical formulation of the model after minimizing the loss according to Equation 1, which, in this particular case, predicts stress as a function of strain rate and strain ($\sigma(\dot{\varepsilon},\varepsilon)$); Unknown coefficients of Equations 3, 4 and 5 (a_0, a_1, c_0 and c_1) and the unknown residual function from Equation 6 $f^*(\dot{\varepsilon},\varepsilon)$ are given in Table 2.

Model	Equation
SR	$\sigma(\dot{\varepsilon},\varepsilon) = 36.661926 - (-123.20189\varepsilon \cdot \sin(0.13883594\varepsilon - \sin(\varepsilon)) + e^{4.032475 - 0.4550452e^{\varepsilon}})$
Baseline	$\sigma(\dot{\varepsilon},\varepsilon) = 20.066474 - 0.864957 \log \dot{\varepsilon} \cdot \varepsilon \cdot e^{-\frac{\varepsilon}{4.051567 + 20.176602\dot{\varepsilon}}}$
Hybrid	$f^*(\dot{\varepsilon},\varepsilon) = \frac{1}{0.2789267} \cdot \sin\left(\frac{\dot{\varepsilon}}{0.009915561} + \sin(\varepsilon)\right)$

Table 2. The discovered and fitted strain stress models

All models are evaluated using standard goodness of fit metrics Mean Squared Error (MSE), Mean Absolute Error (MAE) and Coefficient of Determination (R^2). Overall results as well as the per strain rate values are given in Table 3.

Metric/Model		SR	Baseline	Hybrid
MSE	Overall	3.361	8.906	**3.044**
	$\dot{\varepsilon} = 0.0005\ s^{-1}$	3.007	7.478	2.246
	$\dot{\varepsilon} = 0.002\ s^{-1}$	2.635	7.527	2.785
	$\dot{\varepsilon} = 0.02\ s^{-1}$	6.004	11.425	5.689
	$\dot{\varepsilon} = 0.1\ s^{-1}$	1.597	9.252	1.312
MAE	Overall	1.518	2.452	**1.325**
	$\dot{\varepsilon} = 0.0005\ s^{-1}$	1.544	2.311	1.335
	$\dot{\varepsilon} = 0.002\ s^{-1}$	1.290	1.980	1.201
	$\dot{\varepsilon} = 0.02\ s^{-1}$	2.149	3.114	1.752
	$\dot{\varepsilon} = 0.1\ s^{-1}$	1.024	2.382	0.967
R^2	Overall	0.976	0.936	**0.978**
	$\dot{\varepsilon} = 0.0005\ s^{-1}$	0.961	0.903	0.971
	$\dot{\varepsilon} = 0.002\ s^{-1}$	0.973	0.923	0.971
	$\dot{\varepsilon} = 0.02\ s^{-1}$	0.959	0.921	0.961
	$\dot{\varepsilon} = 0.1\ s^{-1}$	0.994	0.963	0.995

Table 3. Performance metrics for models

Working Paper of 37th DAAAM Symposium

From Table 3, it can be seen that all models achieve a good fit, with low values of MSE and MAE and R^2 values close to 1, with the hybrid model performing best across all metrics. All models appear to predict the highest strain rate curve 0.1 s^{-1} most accurately. Interestingly, the moderate strain rate curve 0.02 s^{-1} is the most difficult to predict. This may be attributed to its transitional shape between the deformation responses observed at lower and higher strain rates. At 0.02 s^{-1}, the pronounced maximum stress characteristic of the lower strain rate curves is no longer clearly present, while the curve has not yet fully developed the smoother post-peak response observed at the higher strain rate. Consequently, the 0.02 s^{-1} curve exhibits a less distinctive shape, making it more difficult for the models to capture the changes in slope and the transition from the pre-peak to the post-peak regime accurately.
The scatter plot of actual stress measurements over the model predictions for all three models is shown in Fig. 3.

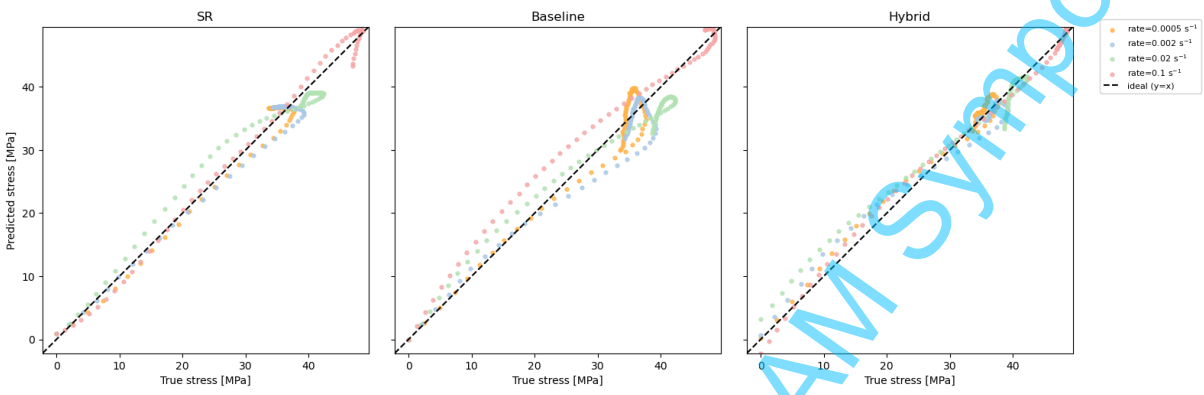

Fig. 3. Actual vs predicted stress

We used the actual measurements and not the interpolated values. The different strain rates are coloured to examine the per strain rate model predictive abilities. It can be seen that all models perform well in the low to middle stress region, as a result of the materials linear behaviour and well captured transition. Similarly, all models perform the best when predicting the high strain rate $\dot{\varepsilon} = 0.1$ s^{-1} curve. The baseline model performs the worst across the whole range of true stress, with the hybrid model performing the best. All models performed worse around the maximum stress region with the hybrid model ameliorating the problem, although not fully. The model predictions could be further improved by allowing for more complex functional formulations during optimization but at the cost of interpretability.
The predicted strain stress curves together with the actual measured curves for all three models and for all four strain rates are shown in Fig. 4.

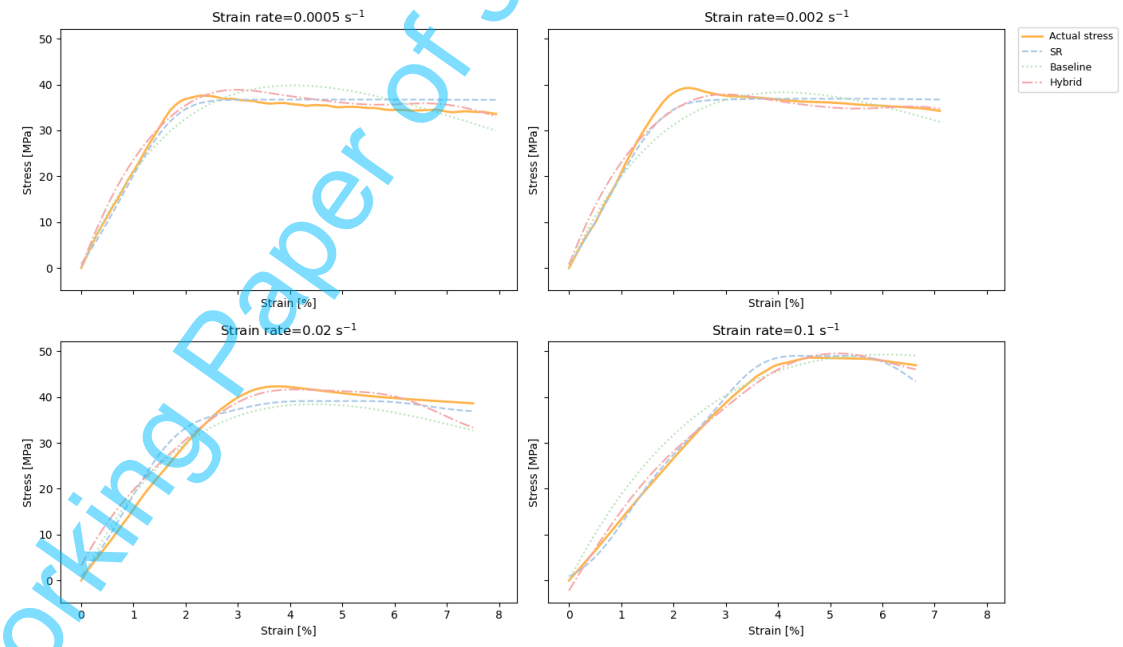

Fig. 4. Predicted and actual strain stress curves

All models are able to capture the general shape of the true relationship, with the hybrid model providing the best overall fit. However, all models slightly underpredict the maximum stress for the $\dot{\varepsilon} = 0.002$ s^{-1} curve. This curve exhibits a

Working Paper of 37th DAAAM Symposium

particularly pronounced maximum stress point compared with the other curves. The hybrid model is not fully capable of accurately predicting the magnitude of the peak while simultaneously correcting the baseline behaviour. In comparison, for the low $\dot{\varepsilon} = 0.0005$ s^{-1} and high $\dot{\varepsilon} = 0.02$ s^{-1} strain rate curve, hybrid model is much more capable of applying necessary correction and accurately predicting the maximum stress.
It would be beneficial to further examine the region around $\dot{\varepsilon} = 0.002$ s^{-1} to determine at which strain rate the transition in curve shape occurs and the pronounced peak stress begins to emerge.

4. Conclusion

This study investigated strain rate-dependent tensile behaviour of FFF-printed Strongman (STR) material at four strain rates ranging from 0.0005 to 0.1 s^{-1}. A hybrid constitutive modelling approach was developed by combining a modified Cingara-based baseline formulation with symbolic regression. Instead of replacing complete constitutive equation, symbolic regression was used to identify a correction term based on residuals between experimental response and baseline model. This resulted in an explicit formulation for stress as a function of strain and strain rate.
Results show that hybrid model provides the best overall agreement with experimental data. Hybrid model achieved an overall MSE of 3.044, MAE of 1.325 and R^2 of 0.978. It also provided the lowest error for most individual strain rates. Highest strain rate of 0.1 s^{-1} was predicted with highest accuracy, while 0.02 s^{-1} curve was most difficult to reproduce. This behaviour can be related to transitional shape of stress strain curve at this strain rate. Hybrid model also improved prediction around maximum stress compared with baseline model. It achieves high prediction accuracy while maintaining some level of physical interpretability within the investigated parameter domain. Symbolic regression therefore provides a balance between predictive accuracy and model interpretability.
Main limitations are related to available experimental data and complexity of material response. Model was developed using four strain rates and its performance is therefore limited to investigated range. Although the closed-form symbolic expression provides an explicit and interpretable mathematical representation of the material response, its extrapolation beyond the tested strain rate range requires further experimental verification. Region around 0.02 s^{-1} remains difficult to describe because of transition in curve shape. In addition, maximum stress region is not captured with same accuracy as rest of response. Increasing complexity of symbolic expression could improve this prediction, but this would reduce model interpretability.
Further research should investigate additional strain rates, with particular attention to region around 0.002-0.02 s^{-1}. This could help determine strain rate at which change in curve shape and pronounced peak stress develop. Implementation of developed formulation in finite element simulations would provide an opportunity to assess its performance for FFF-printed STR components under different loading conditions.

5. References

[1] Ngo, T. D.; Kashani, A.; Imbalzano, G.; Nguyen, K. T. Q.; Hui, D. (2018). Additive manufacturing (3D printing): A review of materials, methods, applications and challenges, Composites Part B: Engineering, Vol. 143, pp. 172–196. DOI:10.1016/j.compositesb.2018.02.012
[2] Gibson, I.; Rosen, D.; Stucker, B.; Khorasani, M. (2021). Additive Manufacturing Technologies, Springer International Publishing, Cham. DOI:10.1007/978-3-030-56127-7
[3] Afshar, R.; Jeanne, S.; Abali, B. E. (2023). Nonlinear Material Modeling for Mechanical Characterization of 3-D Printed PLA Polymer With Different Infill Densities, Applied Composite Materials, Vol. 30, No. 3, pp. 987–1001. DOI:10.1007/s10443-023-10122-y
[4] Hodzic, D.; Pandzic, A.; Hajro, I.; Tasic, P. (2020). Strain Rate Influence on Mechanical Characteristics of FDM 3D Printed Materials, B. Katalinic (Ed.), DAAAM Proceedings (1st edn, Vol. 1), DAAAM International Vienna, 0168–0175. DOI:10.2507/31st.daaam.proceedings.022
[5] Rowland, B.; Jolley, D.; Bennett, B.; Johnson, B.; Moffett, G.; Adair, L.; Hanning-Lee, M.; Bottelberghe, G.; Mamo, T.; Kaufman, J. (2010). Test method and simple analysis model for off-gassing studies of military-relevant surfaces contaminated with chemical warfare agent simulants, Polymer Testing, Vol. 29, No. 7, pp. 777–783. DOI:10.1016/j.polymertesting.2010.06.006
[6] Múgica, J. I.; Aretxabaleta, L.; Ulacia, I.; Aurrekoetxea, J. (2016). Rate-dependent phenomenological model for self-reinforced polymers, Composites Part A: Applied Science and Manufacturing, Vol. 84, pp. 96–102. DOI:10.1016/j.compositesa.2016.01.002

Working Paper of 37th DAAAM symposium

[7] Ibrulj, J.; Obucina, M.; Dzaferovic, E. (2020). Modeling of Viscoelastic Behavior of 3D Printed Polimeric Materials, B. Katalinic (Ed.), DAAAM Proceedings (1st edn, Vol. 1), DAAAM International Vienna, 0328–0333. DOI:10.2507/31st.daaam.proceedings.046

[8] Kabliman, E.; Kolody, A. H.; Kronsteiner, J.; Kommenda, M.; Kronberger, G. (2021). Application of symbolic regression for constitutive modeling of plastic deformation, Applications in Engineering Science, Vol. 6, pp. 100052. DOI:10.1016/j.apples.2021.100052

[9] Kronberger, G.; Kabliman, E.; Kronsteiner, J.; Kommenda, M. (2022). Extending a physics-based constitutive model using genetic programming, Applications in Engineering Science, Vol. 9, pp. 100080. DOI:10.1016/j.apples.2021.100080

[10] Mao, F.; Wang, X.; Li, X.; Shi, R.; Cheng, K.; Wang, Y.; Chen, C.; Yu, H.; Wei, S. (2026). A physics-guided GA-BP neural network constitutive model and hot deformation behavior of 12Cr2Mo1V steel, Journal of Materials Research and Technology, Vol. 43, pp. 5425–5447. DOI:10.1016/j.jmrt.2026.07.097

[11] Abdusalamov, R.; Hillgärtner, M.; Itskov, M. (2023). Automatic generation of interpretable hyperelastic material models by symbolic regression, International Journal for Numerical Methods in Engineering, Vol. 124, No. 9, pp. 2093–2104. DOI:10.1002/nme.7203

[12] Pandzic, A.; Hodzic, D. (2022). Tensile Mechanical Properties Comparation of PETG, ASA and PLA-Strongman FDM Printed Materials With and Without Infill Structure, B. Katalinic (Ed.), DAAAM Proceedings (1st edn, Vol. 1), DAAAM International Vienna, 0221–0230. DOI:10.2507/33rd.daaam.proceedings.031

[13] Hamzic, K.; Pandzic, A. (2026). Strain-Rate Dependent Mechanical Behaviour and Constitutive Modelling of FFF-Printed Strongman and SLA-Printed Flexible 80A, DAAAM Proceedings, DAAAM International Vienna, unpublished

[14] Makke, N.; Chawla, S. (2024). Interpretable scientific discovery with symbolic regression: a review, Artificial Intelligence Review, Vol. 57, No. 1, pp. 2. DOI:10.1007/s10462-023-10622-0

[15] Cranmer, M. (2023). Interpretable Machine Learning for Science with PySR and SymbolicRegression.jl, arXiv. DOI:10.48550/ARXIV.2305.01582

[16] Kabliman, E.; Kronberger, G. (2026). Identification of empirical constitutive models for age-hardenable aluminium alloy and high-chromium martensitic steel using symbolic regression, Philosophical Transactions of the Royal Society A: Mathematical, Physical and Engineering Sciences, Vol. 384, No. 2317, pp. 20240587. DOI:10.1098/rsta.2024.0587

[17] Bahmani, B.; Sun, W. (2023). Physics-constrained symbolic model discovery for polyconvex incompressible hyperelastic materials, arXiv. DOI:10.48550/ARXIV.2310.04286

[18] Cingara, A.; McQueen, H. J. (1992). New formula for calculating flow curves from high temperature constitutive data for 300 austenitic steels, Journal of Materials Processing Technology, Vol. 36, No. 1, pp. 31–42. DOI:10.1016/0924-0136(92)90236-L

Working Paper of 37th DAAAM Symposium